AGRICULTURAL
SCIENCE & TECHNOLOGY

Open Access

Article

Biodegradable Kraft Lignin-Based Agro Hydrogels for Soil Hydration and Slow Release of Urea

Nataliia Fihurka and Tetyana Budnyak*

ABSTRACT: Natural polymer-based hydrogels hold significant potential for sustainable agriculture by enhancing soil hydration and enabling the controlled release of nutrients. This study shows an easy synthetic approach to substitute up to 75% of commonly used polyacrylamide (PAAm) for commercial agro hydrogels by kraft lignin, keeping swelling performance on the same level. A new semisynthetic hydrogel has been synthesized via cross-linking of kraft lignin produced via the LignoBoost process (LB) with PAAm. The ratio of LB and PAAm in the hydrogel composition and cross-linking density were optimized to obtain hydrogels with suitable performance properties. Hydrogel samples were characterized by thermogravimetric analysis, differential scanning calorimetry, and Fourier transform infrared (FTIR) spectroscopy to evaluate the main characteristics and suggest possible reaction mechanisms and by scanning electron microscopy to study features of the hydrogel network. The investigation of functional properties demonstrated that optimized hydrogel samples with 60% lignin in the composition possess water swelling capacity up to 235 g g^{-1} and can significantly increase the water retention of the soil when 2.5% hydrogel is added to the substrate. Moreover, obtained lignin-derived hydrogels have the ability to retain and slow-release urea fertilizer. Thus, lignin-derived urea formulations ensure the sustained cumulative release of urea within 8 days under laboratory conditions, while unencapsulated urea possesses a cumulative release of 97% within 1 h. Investigation of biodegradation using a soil burial test showed that weight loss ranges from 9.5% to 14.5% after 40 days for different hydrogel samples. The proposed method of synthesis of lignin-based hydrogels opens new frontiers in advancing sustainable agricultural technologies.

KEYWORDS: *kraft lignin, polyacrylamide, hydrogel, water retention, slow release of urea*

INTRODUCTION

A global food crisis remains a huge challenge for mankind. WFP (World Food Program) reports that, in 2023, more than 300 million people will face acute levels of food insecurity and more than 700 million will suffer from chronic hunger. Extreme weather conditions, particularly drought, are one of the three main reasons for promoting food crises and global hunger.

This issue and the continuous growth of Earth's population enhance a search for new and improved practices for sustainable agriculture. This topic is mainly related to effective water management and reasonable utilization of fertilizers for a high crop yield.

In the 1980s, synthetic hydrogels as a class of superabsorbent polymers were proposed for agricultural purposes. A cross-linked network of hydrogels showed an excellent ability to absorb high amounts of water with the following prolonged water desorption. The utilization of hydrogels has exhibited numerous advantages for enhanced farming practices, in particular, increased water-holding capacities of soils, allowing the avoidance of drought stress, increased soil porosity (due to the swelling/deswelling cycles of hydrogel particles in the soil), facilitating ventilation and oxygenation to the seed and plant roots,[1,2] and reduced soil erosion and water runoff.[3] Moreover, new hydrogel-based composites for the slow release of nutrients were designed for more efficient uptake and reduced leaching of fertilizers, allowing the utilization of nutrients without excess amounts.[4,5] All of these features provided significant preservation of soil fertility and ecosystem health while using hydrogels as a part of general farming practices.

Up to date, most commercial hydrogels currently available on the market are based on synthetic polymers of polyacrylamide, poly(acrylic acid), or sodium and potassium polyacrylate. Although these synthetic copolymers possess high swelling capacities, they also represent a severe risk of environmental contamination.[6] In terms of sustainability and cost efficiency, biomass and biopolymers are the most promising starting materials for hydrogel production. Therefore, over the last two decades, extensive efforts have been applied to find promising and sustainable approaches to biomass-derived hydrogels. Numerous studies on new hydrogels are based on cellulose,[7−9] starch,[10−12] alginate,[13,14] gelatin,[15,16] pectin,[17] and chitosan.[18,19] However, currently, only one semisynthetic hydrogel is commercially available on the market, and it is composed of cellulose and anionic polyacrylate.[20] This fact promotes further research in this

Received: January 24, 2025
Revised: May 25, 2025
Accepted: May 28, 2025

direction and searches for suitable solutions for the topic of agriculture hydrogels.

One of the most promising candidates as a building block for various materials is lignin, which is emerging as a crucial component in sustainable bioeconomy owing to its abundance in plant cell walls.[21] Despite its historical role primarily as a waste byproduct of pulping processes, recent advancements have unveiled lignin's potential as a renewable resource for biofuels, chemicals, and materials.[22−25]

The most widespread type of lignin is kraft lignin deriving from the kraft pulping process, which is the dominant method for producing pulp from wood for papermaking worldwide.[26,27] This process accounts for a significant portion of global pulp production, particularly in Nordic regions, where softwood species such as pine and spruce are abundant, causing the production of millions of tons of kraft lignin annually. Its versatile chemical properties and relatively low cost compared to other types of lignin make it a preferred choice for various industrial applications beyond papermaking.[27,28]

Zerpa et al.[29] reported hydrogels based on hardwood kraft lignin and *N*-isopropylacrylamide cross-linked by *N*,*N*′-methylenebis(acrylamide) via radical polymerization using azobis(isobutyronitrile) as an initiator at 65−85 °C. The obtained hydrogel showed higher thermal stability but a lower specific surface area and more porous structure than the synthetic one, which provoked a decreased maximum swelling capacity of 33 g H_2O g^{-1}, which is low compared to synthetic hydrogels. Moreover, the composition of the proposed hydrogels consists of only 5% lignin and 95% *N*-isopropylacrylamide.

The multistep synthetic approach suggested by El-Zawawy et al.[30,31] increased the content of lignin in the final hydrogel. At the first stage, poly(vinyl alcohol) and acrylamide were grafted to kraft lignin via free emulsion polymerization initiated by potassium persulfate. Then, grafted lignin and acrylamide were cross-linked using the redox initiators potassium persulfate and sodium metabisulfite under an inert atmosphere at room temperature for 24 h. Despite the complex synthetic approach, obtained hydrogel samples possess even lower swelling capacity of 6 g H_2O g^{-1}.

Farhat et al.[32] proposed reactive extrusion for hydrogels based on kraft lignin and citric acid using sodium hypophosphite as a catalyst. Hydrogel production was performed at the residence time in the extruder from 2 to 5 min of recirculation, a screw rotation speed of 120 rpm, and a temperature of the extruder at 120 °C. The same approach was used for hydrogels based on starch, hemicellulose, and lignin, which showed the lowest swelling capacity, up to 4.5 g H_2O g^{-1}.

Even though significant advances have been recently made in the area of design and synthetic approaches for lignin-derived hydrogels, their commercialization and industrial production remain challenging due to the high cost of manufacturing and complex production processes. Thus, it is crucial to develop green protocols for kraft lignin-based hydrogels corresponding to sustainability and circular economy principles.

This work aimed to synthesize a series of lignin-based hydrogels with different compositions and cross-linking degrees prone to high swelling capacity, water retention, and the ability to sustain fertilizer release. Therefore, highly hydrophilic polyacrylamide was used as a copolymer for composite hydrogels. Afterward, the obtained semisynthetic hydrogels were loaded with urea to form fertilizer formulation for sustained release. The impact of hydrogel composition and structure on swelling properties, urea release patterns, and other performance characteristics have been investigated.

MATERIALS AND METHODS

Materials. Kraft lignin obtained by the Lignoboost process from softwood (LB395) was supplied by UPM BioPiva, Finland. Polyacrylamide (average M_m of 300 kDa) was obtained from Sigma-Aldrich and used as received. Formaldehyde (aqueous solution, 37 wt %, biotechnology grade) was obtained from Amresco and used as received.

Methods. *Hydrogel Preparation.* Lignin was mixed with deionized water and 1 M KOH (water:1 M KOH = 2.5:1 v:v) and stirred for 15 min at 300 rpm to fully dissolve. Then, certain amounts of polyacrylamide (4:6 w:w of PAAm to lignin) and formaldehyde (0.042 or 0.062 g g^{-1} of lignin) were added with continuous stirring. The total concentration of reagents in the reaction mixture was 10 wt %. After being stirred for another 30 min, the reaction mixture was maintained at 70 °C for 72 h. Finally, hydrogel samples were freeze-dried for 24 h. As such, samples LB60/PAAm40/FA0.042 and LB60/PAAm40/FA0.062 were synthesized. Dry hydrogel samples were weighed and subjected to two cycles of swelling and deswelling to estimate the amount of sol and gel fraction.

Fourier Transform Infrared (FTIR) Spectroscopy. Spectra were recorded with a Bruker Tensor 27 ATR-FTIR Spectrometer (Bruker) on dried pellets prepared by pressing the mixture of LB or ground into powder hydrogel samples (3 mg) and 200 mg of KBr under 8 tons. The FT-IR spectra were recorded using 32 scans between 500 and 4000 cm^{-1} with a resolution of 4 cm^{-1}. All samples were freeze-dried.

Differential Scanning Calorimetry (DSC). DSC of initial lignin, polyacrylamide, and hydrogel samples was performed with a DSC 204 F1 instrument (Netzsch-Gerätebau GmbH). Each sample (6 to 7 mg) was weighed into a standard aluminum pan (40 μL) and heated under a nitrogen atmosphere with a flow rate of 15 mL min^{-1}. The sample was initially heated to 200 °C at a rate of 10 °C min^{-1}. Next, the sample was cooled to −10 °C at a rate of 30 °C min^{-1}. Finally, the sample was reheated to 270 °C at a rate of 10 °C min^{-1}. The initial heating and cooling cycles were carried out to clear the thermal history of the sample to eliminate the endothermic enthalpy relaxation that usually affects the T_g determination.[33] The T_g value of each sample was measured from the last heating cycle.

Thermal Gravimetric Analysis (TGA). TGA of initial kraft lignin, polyacrylamide, and hydrogel samples was performed on a TGA/DSC/IR (Mettler Toledo, Columbus, OH, USA) instrument under the following operational conditions: a heating rate of 10 °C min^{-1}, a dynamic atmosphere of air or nitrogen (50 mL min^{-1}), a temperature range of 30−900 °C, and a sample mass of 2.5 mg. The derivate maximum decomposing rate temperature (DTG_{max}) and the corresponding weight loss as well as the residual mass were determined. The measurements were performed in duplicate.

Molecular Weight Analysis of Initial Kraft Lignin. The molecular weight of acetylated lignin prepared according to the procedure in ref 34 was analyzed using a Hitachi HPLC Chromaster system equipped with two LC Phenogel columns 50 Å and 500 Å (5 μm, 7.8 × 300 mm each and flow rate of 1 mL min^{-1}) connected in series and with a UV detector (280 nm). The calibration was performed using ReadyCal-Kit polystyrene (266, 682, 1250, 2280, 3470, 4920, 9130, 15700, 21500, 28000, 44200, 66000 g mol^{-1}). The values of M_n and M_w were calculated using Clarity Chromatography Software.

^{31}P NMR Analysis of Initial Kraft Lignin. Quantification of lignin functional group content was performed using the procedure described by Argyropoulos et al.[35] A ^{31}P NMR spectrum of the phosphorylated sample was recorded using a 400 MHz JEOL solution NMR spectrometer with a relaxation delay of 10 s and 128 scans.

Functional Properties. Swelling in Deionized Water. About 0.1 g of washed and freeze-dried hydrogel samples was weighed and immersed in deionized water for 24 or 48 h. The swelling ratio *W* (g

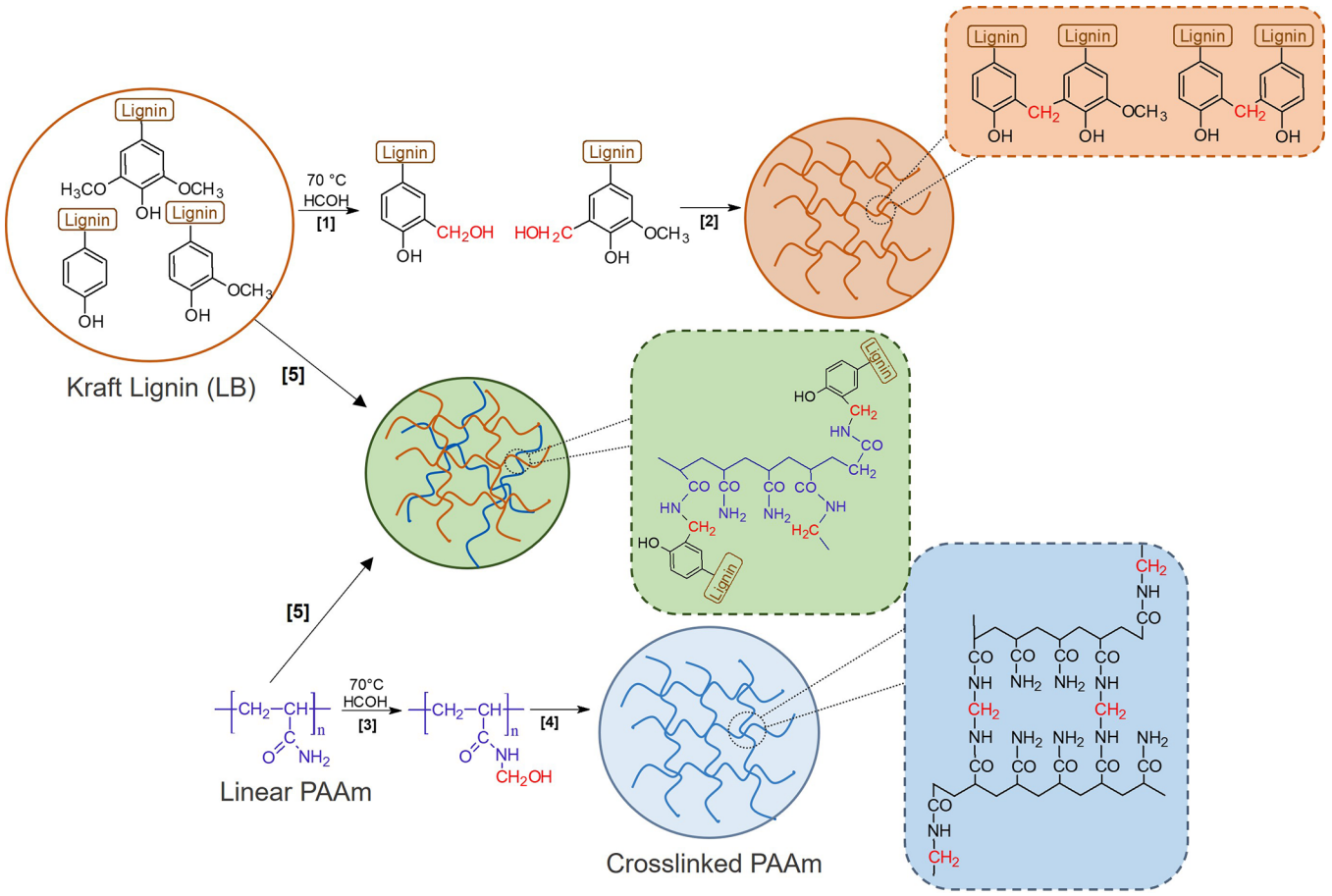

Figure 1. Proposed mechanism for the formation of a hydrogel network based on lignin and linear polyacrylamide.

$H_2O\ g^{-1}$) of hydrogel samples was assessed by comparing the weight of the swollen sample m_s and the weight of the dried sample m_d according to the following equation:

$$W = \frac{m_s - m_d}{m_d} \quad (1)$$

The data was obtained and reported as an average of triplicates.

The swelling kinetics were explored by determining the swelling ability of 0.1 g freeze-dried hydrogel samples in deionized water at various immersion intervals, and the swelling ratios at a certain time t (W_t, g $H_2O\ g^{-1}$) were determined using eq 1.

The swelling kinetic models were used to investigate the swelling behavior further. The kinetic data were fitted using the Fickian model (first kinetic order) (eq 2)[36,37] and the Shott model (pseudo-second kinetic order) (eq 3).[38]

$$\frac{W_t}{W_e} = kt^n \quad (2)$$

where k is a constant characteristic of the system and n is the diffusion exponent affected by the water transport mechanism, W_t is the swelling ratio at time point t, and W_e is the equilibrium swelling ratio.

$$\frac{t}{W_t} = \frac{1}{k_{in}} + \frac{1}{W_\infty}t \quad (3)$$

where k_{in} is the initial swelling rate of the hydrogel and W_∞ is the theoretical equilibrium swelling ratio.

Water Retention of Hydrogels in Soil. Dried samples (250 mg) were weighed and added to 10 g of dried soil in a 50 mL beaker. At the same time, 10 g of dried soil without hydrogel was placed in another beaker as a control. Then, 20 mL of distilled water was added to each beaker, and the mixture was weighed. The tests were conducted using commercial soil intended for home planting (pH ~ 7). The beakers were maintained at ambient temperature and weighed daily until they reached a constant mass. The water retention Wr (%) of soil was calculated by eq 4.

$$\mathrm{Wr} = \frac{m_i - m_t}{m_o - m_t} \cdot 100\% \quad (4)$$

where m_i is the total mass of sand, beaker, and sample after adding distilled water, m_o is the total mass of sand, beaker, and sample after adding distilled water, m_t is the total mass of sand, beaker, and sample at a certain day of the experiment.

Urea Loading. Dried samples (100 mg) were immersed in a urea solution in distilled water, with urea concentrations ranging from 10 to 40 wt %. The samples were soaked in this solution for 24 h under ambient conditions. Afterward, the samples were thoroughly washed with distilled water and freeze-dried for 24 h. The amount of loaded urea, W_u (g urea g^{-1}), was calculated using eq 5

$$W_u = \frac{m_l - m_d}{m_d} \quad (5)$$

where m_l is a weight of the loaded sample after freeze-drying and m_d is an initial weight of the dried hydrogel sample.

Urea Release. The urea concentration was calculated using para-dimethylamino-benzaldehyde colorimetry. Specifically, 1 mL of the urea solution was added to the mixture of 1.8 mL of the 3 gL^{-1} para-dimethylaminobenzaldehyde solution and 0.065 mL of the 35% HCl. The solution was shaken three times to make the reaction complete and even, followed by a 15 min rest before testing using the UV spectrophotometer at 410 nm wavelength. The UV-absorbance results were calculated by using the standard curve method. The data was obtained and reported as an average of triplicates.

Biodegradation Tests. Soil burial tests were performed to evaluate the biodegradation of lignin-derived hydrogels in soil.[39,40] The test

Table 1. Content of Functional Groups and Molecular Weight of Raw Lignin Material

Sample	Molecular Weight			Content of Functional Groups, mmol g^{-1}			
	M_w, Da	M_n, Da	PDI	Phenolic OH	Aliphatic OH	Total OH	Carboxyl
LB395	3700	1200	3.0	4.03	1.84	5.87	0.24

Table 2. Variables and Their Corresponding Values in the Orthogonal Experimental Design for Lignin-Derived Hydrogel Preparation

No.	Sample Name	Hydrogel Composition		Formaldehyde,[a] g g^{-1}	Swelling Degree 48 h, g g^{-1}	Gel Fraction, %
		LB, wt %	PAAm, wt %			
1.	LB45/PAAm55/FA0.058	45	55	0.0572	173.8 ± 7.4	84.4 ± 2.7
2.	LB50/PAAm50/FA0.036	50	50	0.0355	255.2 ± 9.6	83.3 ± 1.9
3.	LB50/PAAm50/FA0.071	50	50	0.0711	143.0 ± 6.0	88.5 ± 1.5
4.	LB60/PAAm40/FA0.021	60	40	0.0224	450.7 ± 18.5	54.1 ± 2.2
5.	LB60/PAAm40/FA0.042	60	40	0.0423	235.5 ± 10.3	86.4 ± 2.6
6.	LB60/PAAm40/FA0.062	60	40	0.0623	152.4 ± 6.2	84.0 ± 2.5
7.	LB70/PAAm30/FA0.021	70	30	0.0212	406.1 ± 16.8	62.4 ± 1.8
8.	LB70/PAAm30/FA0.042	70	30	0.0425	146.1 ± 5.8	91.0 ± 1.4
9.	LB75/PAAm25/FA0.028	75	25	0.0275	N/A	N/A

[a]Gram of formaldehyde per 1 g of copolymers (lignin and polyacrylamide).

was conducted using commercial soil intended for home planting (pH ~ 7). Briefly, 500 mg of a dried hydrogel sample was placed in plastic recipients with soil at a burial depth of 5 cm. At different time points (10, 25, 35, 45, and 55 days), the samples were removed from the soil, rinsed with deionized water, frozen, and lyophilized for 24 h for further analysis. Biodegradation was evaluated based on mass loss. The test was performed in triplicate at each time point. The dried mass of the samples before (W_0) and after (W_t) the degradation test was recorded for gravimetric assessment and the weight loss (WL) at a given time was calculated using eq 6.

$$\mathrm{WL} = \frac{W_0 - W_t}{W_0} \cdot 100\% \tag{6}$$

Viscoelastic Properties of Lignin-Derived Hydrogels. The rheological characterization of the hydrogel samples was performed using a Discovery HR-3 Hybrid instrument (TA Instruments) equipped with a parallel plate geometry (20 mm diameter). Hydrogels with a high of 2000 μm were loaded onto the Peltier plate; the geometry was lowered until a constant axial force of 0.2 ± 0.1 N was achieved, ensuring continuous contact between the geometry and the hydrogel. Samples were allowed to equilibrate for 120 s before the start of the procedure, and all experiments were performed at 20 °C in the oscillatory mode. First, an amplitude sweep from 0.01% to 100% strain at 1 Hz oscillation frequency was conducted to determine the linear viscoelastic region (LVR) of the sample, where stress and strain are proportional (Figure 1, SI). A strain of 0.25% was selected to evaluate the frequency dependence of the dynamic moduli G' and G''. After that, a frequency sweep from 0.01 to 10 Hz at 0.25% strain was performed, and the frequency dependence of the storage (G') and loss (G'') modulus was evaluated as the indicator of the viscoelastic response of the lignin-derived hydrogels.

RESULTS AND DISCUSSION

Different types of lignin include various ratios of phenylpropane units and, therefore, have different molecular masses and an abundance of functional groups such as methoxy, hydroxyl, carboxyl, and carbonyl groups. This variability in structure and functionality is crucial for determining lignin's suitability for various applications, including its use as a renewable resource in biobased materials.

In the current study, a kraft-lignin-derived hydrogel for agriculture applications was prepared using lignin produced via the lignoboost process, with characteristics given in Table 1. The chosen type of lignin possesses an average level of polydispersity index, confirming the broad distribution of molecular weights along with a branched structure of lignin macromolecules. However, this lignin type has a high content of functional groups compared to other softwood lignins,[41,42] making it a promising candidate for chemical modifications.

The proposed synthetic approach utilizes formaldehyde as a cross-linking agent and two components—lignin and polyacrylamide—to form a hydrogel network. It consists of several reactions co-occurring in the reaction mixture (Figure 1). Both lignin and polyacrylamide can react with formaldehyde in alkaline media. In the case of polyacrylamide, the reaction may occur on each amide group of the polyacrylamide chain,[43,44] giving poly(*N*-methylol acrylamide) (reaction 3, Figure 1). In contrast, as a polyphenolic compound, lignin can react with formaldehyde only in ortho and para positions[45] to hydroxyl groups (reaction 1, Figure 1). Other functional groups often block these positions. Moreover, lignin has a highly branched network based on substituted phenolic rings, causing additional steric hindrance. These two obstacles suggest that the formation of methylated lignin in this system is less favorable than the formation of poly(*N*-methylol acrylamide). However, lignin is partially cross-linked according to reaction 2 (Figure 1) when formaldehyde forms cross-linking points between lignin macromolecules. Another route for methylated lignin is the interaction with the amide group of polyacrylamide (reaction 5, Figure 1), forming a covalent bond between lignin and polyacrylamide macromolecules.

The formation of methylol groups in the polyacrylamide chain (reaction 3, Figure 1) is reversible as the oxygen atom of the methylol group has high nucleophilicity and induces a displacement reaction releasing formaldehyde.[46] Thus, polyacrylamide cross-linking (reaction 4, Figure 1) occurs via an interaction between the methylol groups and the intact amide groups or the amide groups produced in the displacement process. Finally, methylol groups of polyacrylamide interact with lignin aromatic rings to form cross-linking bridges and, as a result, cross-linked hydrogel networks were formed.

According to the discussion above, we suggest that the dominant reactions in this system are (i) the cross-linking of polyacrylamide according to reaction 4, Figure 1 and (ii) the

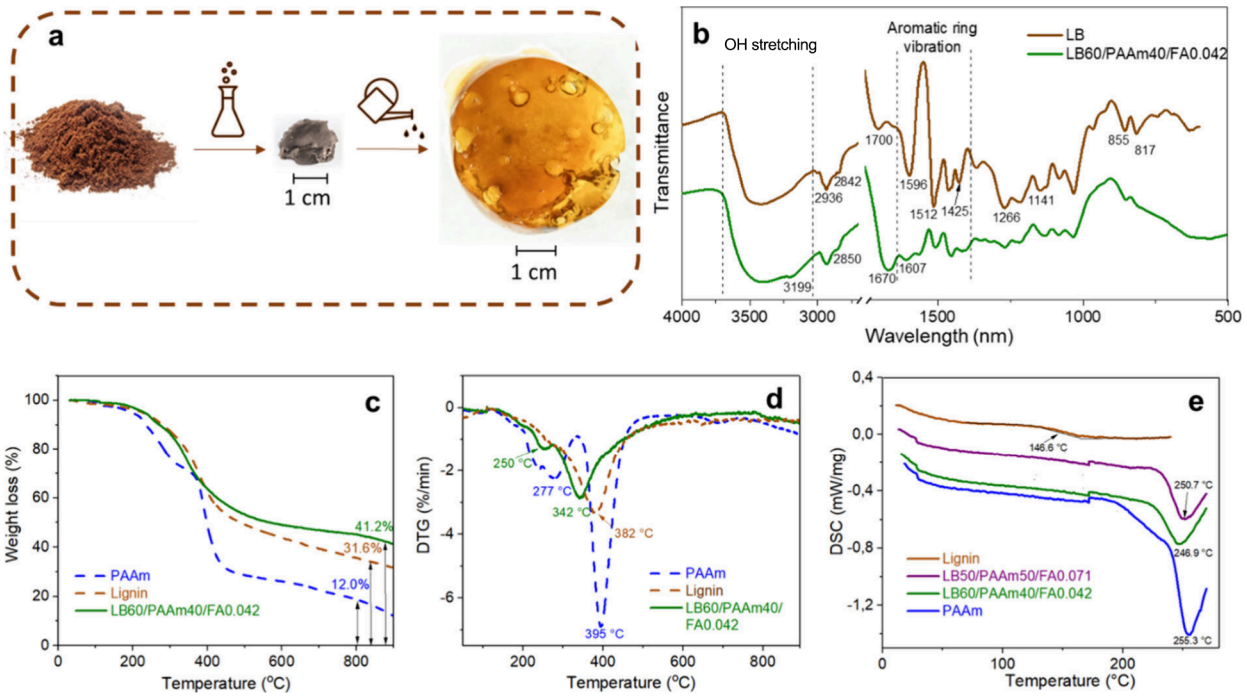

Figure 2. (a) Photographs of raw lignin, dried and swollen lignin-based hydrogels; (b) FTIR spectra of intact lignin LB and LB60/PAAm40/FA0.042 hydrogel; TG (c) and DTG (d) curves of intact lignin LB, PAAm, and lignin-derived hydrogel LB60/PAAm40/FA0.042; (e) DSC thermograms of the intact lignin, lignin-derived hydrogels LB50/PAAm50/FA0.071 and LB60/PAAm40/FA0.042, cross-linked PAAm.

cross-linking of polyacrylamide with lignin according to reaction 5, Figure 1.

The orthogonal plan was built to investigate the optimal lignin:PAAm ratio and the amount of cross-linking agent to obtain an optimal number of cross-linking points. Table 2 presents the applied ratio for the synthesis of hydrogel samples. The content of LB and PAA and the amount of formaldehyde added were determined as three experimental factors of orthogonal tests, and each factor had three levels. Two factors were chosen to evaluate the efficiency of the process: (i) the swelling degree indicating the perspective of the obtained material for agriculture purposes and (ii) the gel fraction content revealing the reaction conditions with the highest efficiency for raw material utilization.

The orthogonal design led to the optimized combinations (samples LB60/PAAm40/FA0.062 and LB60/PAAm40/FA0.042) through 9 experiments (Figure 2a).

Sample 7 (Table 2) has the highest swelling degree and only 30% of synthetic PAAm in the hydrogel composition, which makes it a valuable candidate as a sustainable value-added material. However, this hydrogel sample has a low content of gel fraction (62.4%) and loses its integrity at high values of swelling degree. Sample 8, with the same copolymer composition but a two times higher amount of added cross-linking agent, possesses an acceptable level of gel fraction (83.3%) and remains self-standing gel at equilibrium swelling degree after 48 h. However, this sample has significantly decreased swelling capacity compared to sample 7 (146.1 g g^{-1} vs 406.1 g g^{-1}).

Samples 2 and 3, with equal amounts of lignin and PAAm, have a similar correlation between the amount of formaldehyde added to the system and hydrogel properties, confirming the crucial effect of cross-linking density on swelling capacity and gel fraction. Samples with 60% lignin and 40% PAAm (nos. 4–6) possess the aforementioned patterns. Thus, the low cross-linking density of sample 4 provides high swelling capacity but is not enough to grant a proper level of mechanical properties after significant swelling. On the contrary, sample 5, with a higher content of cross-linking points, remains self-standing hydrogel at equilibrium swelling degree and has suitable swelling capacity (235.5 g g^{-1}) and gel fraction content (86.4%). It is worth mentioning that sample 8, with a similar amount of formaldehyde per 1 g of initial copolymer but a 10% higher content of lignin in the hydrogel composition compared to sample 5, has alike gel fraction content but significantly decreased swelling capacity, indicating a strong impact of lignin fragments on the ability of the hydrogel network to diffuse and retain water molecules. Hence, samples 5 and 6, LB60/PAAm40/FA0.042 and LB60/PAAm40/FA0.062, were selected for the following investigations as candidates with the highest content of lignin and acceptable performance characteristics.

FTIR studies aimed to evaluate which functional groups participate in forming the covalent hydrogel network. The spectra of LB and LB60/PAAm40/FA0.042 hydrogel are presented in Figure 2b.

A broad band centered at around 3400 cm^{-1} is assigned to the hydroxyl stretching of phenolic and aliphatic moieties of lignin. A new peak at 3199 cm^{-1} appearing in this area on the spectra of LB60/PAAm40/FA0.042 hydrogel can be attributed to the symmetric stretching of the amide bond of polyacrylamide.[47] Characteristic bands at 2936 cm^{-1} and 2842 cm^{-1} arise from C–H stretching of the methoxyl group conjugated with aromatic rings and methyl and methylene groups of the lignin side chains. The shoulder at 2850 cm^{-1} appearing at the hydrogel spectrum is attributed to the –N–CH_2– bonds from the cross-linking bridges.[48]

The characteristic bands of aromatic ring vibration are observed at 1596 cm^{-1}, 1512 cm^{-1}, and 1425 cm^{-1}.[49,50] These peaks are partially decreased or vanished in the spectrum of the

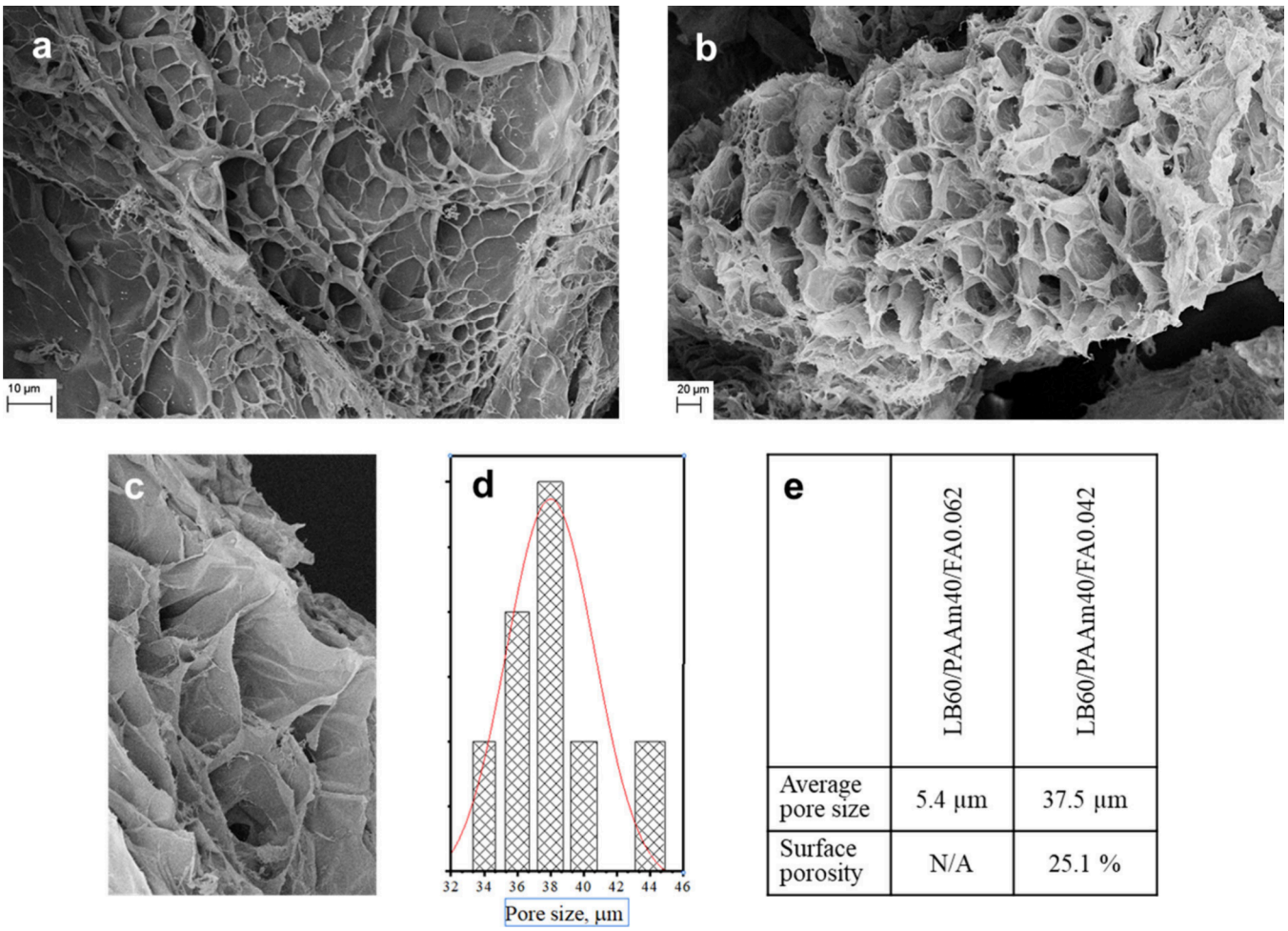

e	LB60/PAAm40/FA0.062	LB60/PAAm40/FA0.042
Average pore size	5.4 μm	37.5 μm
Surface porosity	N/A	25.1 %

Figure 3. SEM images of the freeze-dried hydrogels (a) LB60/PAAm40/FA0.062 and (b) LB60/PAAm40/FA0.042; (c) enlarged SEM image of LB60/PAAm40/FA0.062; (d) distribution of pore size for LB60/PAAm40/FA0.042; (e) summarized data on average pore size and porosity.

LB60/PAAm40/FA0.042 hydrogel, confirming the involvement of the aromatic skeleton in a condensation reaction. Moreover, aromatic C−H out-of-plane deformation vibrations observed at 817 cm^{-1} and 855 cm^{-1} in the LB spectrum almost vanish in the hydrogel spectrum, suggesting modification in position 5 of the guaiacyl units. These findings are consistent with the reaction mechanism proposed in Figure 1. Furthermore, the band at 1700 cm^{-1} assigned to carbonyl stretching of carboxyl groups or ketones in lignins is absent in the hydrogel spectrum, indicating their participation in the cross-linking reaction. The FTIR spectrum of the hydrogel LB60/PAAm40/FA0.042 contains new peaks that arise in this region. In particular, the bands at 1670 cm^{-1} and 1607 cm^{-1} belong to carbonyl stretching vibration (amide I) and NH bending (amide II), confirming the incorporation of polyacrylamide chains into the hydrogel network.[51,52]

To investigate the thermal decomposition of the hydrogel components and the resulting material, thermogravimetric analysis was performed. Figure 2c,d presents TGA and DTG curves for lignin, linear polyacrylamide, and obtained hydrogel LB60/PAAm40/FA0.042. After the initial moisture loss, the intact lignin has one major DTG peak at 382 °C when primary lignin pyrolysis occurs, including processes of lignin fragmentation and release of monomeric phenols. The thermal decomposition profile of polyacrylamide has three steps of weight loss. Below 200 °C, evaporation of adsorbed water occurs. The second stage starts at 210 °C and continues to 335 °C with a DTG peak at 277 °C and weight loss of 22.3% caused by the release of ammonia, water, and minor quantities of CO_2 due to the irreversible intra- and intermolecular imidization reactions at the amide group.[53] The third stage ranges from 345 to 450 °C with a DTG peak at 395 °C. It includes imide decomposition and degradation of the polymeric backbone at higher temperatures resulting in weight loss of 40.1% at this stage and overall residual mass of 12.0% after 800 °C.

The decomposition curve of the obtained hydrogel contains a peak of water evaporation, followed by a DTG peak at 250 °C attributed to the initial decomposition of polyacrylamide. The third peak starts at 250 °C and continues to 550 °C with a DTG peak at 342 °C and can be assigned to both decomposition of polyacrylamide and lignin pyrolysis. The residual mass of the hydrogel sample after 800 °C is 41.2%. Thus, obtained lignin-derived hydrogels showed higher thermal stability than cross-linked PAAm-based hydrogels.[54,55]

The thermal behavior of the lignin-based hydrogels was also evaluated by employing DSC analysis (Figure 2e). The glass transition of lignin is not a formal phase transition; therefore, one can observe a slight change in the DSC heating curve rather than a sharp peak.[56] Thus, a slight change in the DSC curve of intact lignin at 146.6 °C is determined as T_g. The melting point of lignin in the studied temperature range was

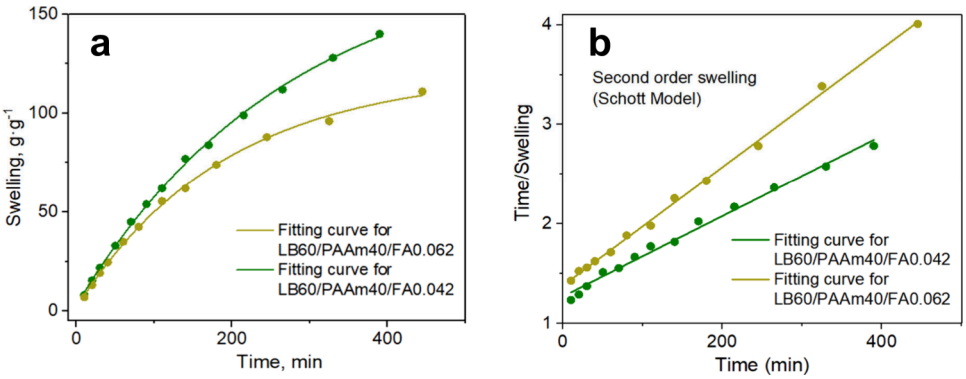

Figure 4. Absorption capacity plots (a) and swelling kinetic fitting curves (b) in deionized water for the first 7 h of incubation.

Table 3. Kinetic Parameters for First-Order and Pseudo-Second-Order Swelling

		Kinetic Model Fitting						
		First-Order			Pseudo-Second-Order			
	Sample name	n	k	R	n	k	R	W_∞, g·g^{-1}
1	LB60/PAAm40/FA0.062	0.7454	−2.186	0.988	0.00595	1.3301	0.997	168.1
2	LB60/PAAm40/FA0.042	0.7744	−2.173	0.993	0.00404	1.1271	0.990	247.5

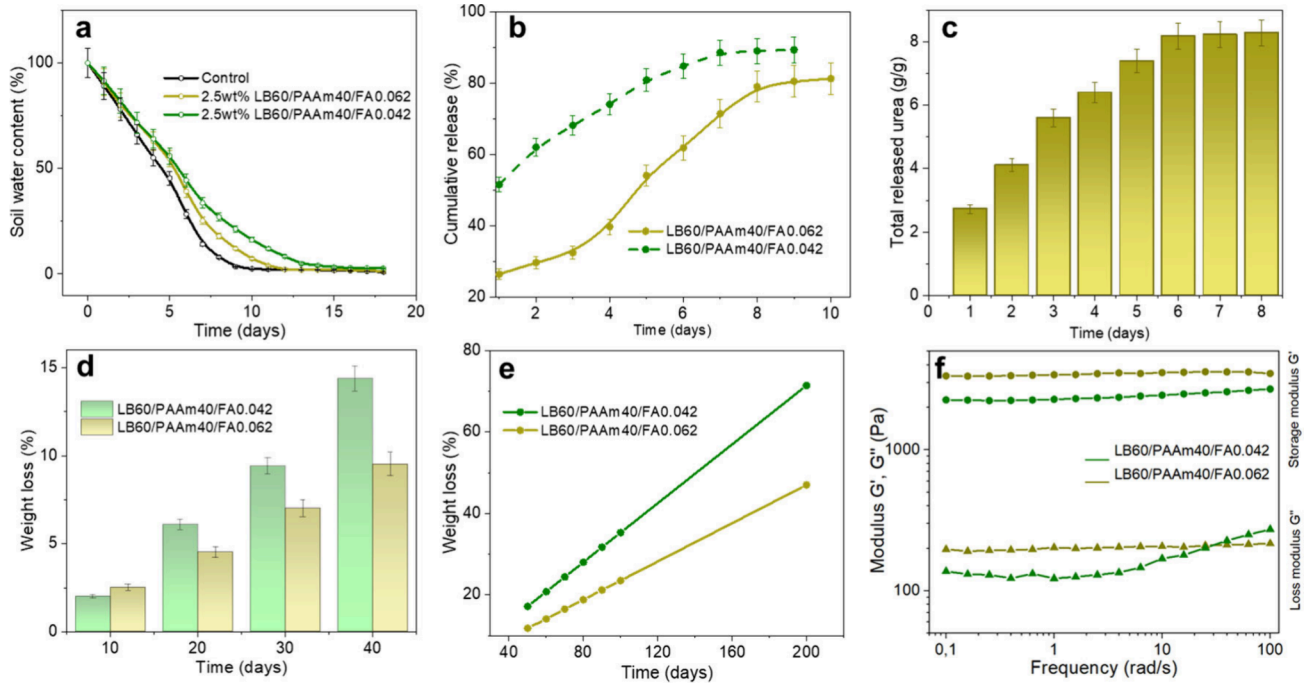

Figure 5. (a) Water content of the soil mixed with lignin-derived hydrogels; (b) urea release curves in static water of LB60/PAAm40/FA0.062 and LB60/PAAm40/FA0.042 hydrogels; (c) total released urea per 1 g of loaded and dried LB60/PAAm40/FA0.062 hydrogel; (d) weight loss of hydrogel samples during incubation in soil for 40 days; (e) linear extrapolation of biodegradation experimental data for 200 days; (f) curves of storage modulus (G') and loss modulus (G'') at the strain of 0.25% LB60/PAAm40/FA0.062 and LB60/PAAm40/FA0.042 hydrogels.

not observed. The DSC profile of PAAm cross-linked in the same conditions as the investigated hydrogels has two major regions. The first one that covers temperatures from 190 to 235 °C is attributed to the glass transition of nonstructured PAAm (sol fraction). The second stage has a sharp peak at 255.3 °C and can be assigned to the glass transition of cross-linked PAAm, which is in agreement with the reported data.[57,58]

For copolymer hydrogels, glass transition temperature is a criterion to determine their miscibility. Hydrogels possessing immiscibility have a broadening of the transition or even two separate peaks for the hydrogel components. Miscible hydrogel systems have a single transition DSC profile. In the case of the obtained hydrogels, DSC curves have one endothermic reaction attributed to glass transition with T_g = 246.9 °C for LB60/PAAm40/FA0.042 and T_g = 250.7 °C for LB50/PAAm50/FA0.071, confirming the mechanism of hydrogel network formation proposed in Figure 1.

The morphology of the lignin-based hydrogel is shown in Figure 3. Although the pore distribution for LB60/PAAm40/

FA0.062 (Figure 3a) is uneven and the average pore diameter porous structure is only 5.4 μm, these pores have a tunable nature (Figure 3c) and provide channels for water transport. The SEM image of LB60/PAAm40/FA0.042 (Figure 3b) illustrates a wide-ranging porous structure with more uniform pore distribution compared with LB60/PAAm40/FA0.062 and narrow distribution of pore size ranging from 34 to 44 μm (Figure 3d). The total porosity of this sample at the given SEM image is 25.1%, making it a promising material for water retention.

The capacity of hydrogel materials for water uptake is one of the most crucial characteristics, in particular for agriculture applications. Exposure to an aqueous medium promotes the formation of hydrogen bonds between functional groups in the hydrogel structure and water molecules, ensuring water penetration into the hydrogel network and causing swelling. To gain a greater understanding of the correlation between hydrogel composition and structure and swelling behavior, equilibrium water uptake and swelling kinetics were studied. Thus, the water absorption of obtained hydrogels reached an equilibrium state within 48 h.

For the swelling characterization, in particular, to determine the nature of water's diffusion into the hydrogel network, the fitting of swelling initial stages to one of the equations describing swelling order was performed. Figure 4a presents the swelling rate for the first 7 h.

Hydrogel systems conform to the Fickian diffusion mechanism (the first kinetic order) when at initial stages ($W_t/W_e \leq 60\%$) of the diffusion constant (eq 2), $n < 0.5$. The data presented (column 3 in Table 3 and Figure S1) reveal that diffusion constant n for studied hydrogel samples lies outside the normal range for the Fickian model, suggesting that in this case the swelling mechanism is not governed exclusively by the diffusion through the porous structure. On the other hand, the plot of experimental data as the curves of the reciprocal of average swelling T/W_t versus time (Figure 4b) gave straight lines with good linear correlation coefficients (column 8, Table 3), suggesting that the swelling process for both hydrogel samples follows a pseudo-second-order swelling kinetic model (Schott Model) and is controlled by the relaxation of polymeric chains in the hydrogel network.

Kinetic parameters k_{it} and W_∞ were calculated based on the slope and intercept values of the fitted curves. The values of W_∞ (Table 3, column 9), which are theoretically maximal swelling capacities, correspond to the experimental values of the equilibrium swelling ratio given in Table 2.

Thus, the swelling patterns of lignin-derived hydrogels correspond to the reported data on cellulose-based hydrogels[59,60] proposed for agricultural applications, suggesting that the obtained hydrogels possess swelling kinetics that meet the requirements for agricultural soil conditioners.

The ability of the obtained hydrogels to retain moisture in the soil compared to the soil sample without hydrogel is presented in Figure 5a. On the first days of incubation, all samples showed similar moisture content loss, i.e., 66% of initial water content for soil without hydrogels and 72% for soil samples containing 2.5 wt % of LB60/PAAm40/FA0.062 and LB60/PAAm40/FA0.042 hydrogels on day 3. On day 7, the soil without hydrogel conditioner contained approximately 14% of initial moisture, while hydrogels LB60/PAAm40/FA0.062 and LB60/PAAm40/FA0.042 increased water retention of soil samples to 25% and 34% correspondingly on the same day. The water content of soil samples without hydrogel completely vaporized after day 9, while soil samples containing hydrogels still had 12% moisture for LB60/PAAm40/FA0.062 and 21% for LB60/PAAm40/FA0.042. Complete drying of hydrogel-containing soil samples was observed on day 12 for LB60/PAAm40/FA0.062 and day 16 for LB60/PAAm40/FA0.042, confirming the ability of the obtained lignin-derived hydrogels to enhance soil water retention to avoid drought stress for seeds and crops.

Urea is one of the most widely used solid nitrogen fertilizers; therefore, it was chosen to investigate the potential of the obtained lignin-derived materials as controlled-release formulations for agricultural fertilizers. Standard (unencapsulated) urea cumulative release in distilled water reaches 97% within 1 h.[61,62]

Release patterns of urea from the urea-loaded hydrogels with the same composition (60 wt % of lignin and 40 wt % of PAA) but different cross-linking degrees in static water are presented in Figure 5b. The hydrogel with lower cross-linking density LB60/PAAm40/FA0.042 has quite a rapid release profile with 50% urea release on the first day and prolonged release reaching 88% on day 7.

Adversely, a hydrogel with a higher cross-linking density LB60/PAAm40/FA0.062 has a more pronounced profile of urea slow release. The initial stage covers the first 3 days of incubation with 25% of urea released on the first day and 32% on the third day, apparently due to the dynamic exchange of free water.[63] After this, more rapid urea release is observed (days 4−8) with 79% urea cumulative release on day 8 followed by a plateau at about 82%. The urea-releasing profile with three stages with different rates has been reported for other biopolymer-based hydrogel systems.[64]

Thus, hydrogel LB60/PAAm40/FA0.042 with a higher swelling capacity and porosity possesses a higher rate of urea release. Higher swelling promotes the diffusion of water molecules into the hydrogel network, followed by partial breaks of hydrogen bonds between lignin macromolecules and urea. This results in the accelerated diffusion of urea molecules from the hydrogel network into the releasing medium. In contrast, the hydrogel LB60/PAAm40/FA0.062 possesses a more sustained profile for urea release provided by decreased water absorption capacity. This correlation allows one to control parameters of urea slow-release formulations based on the lignin-derived hydrogels via the change in the water swelling capacity and the porosity structure easily adjustable by the number of cross-linking points.

Figure 5c shows the total amount of released urea. Thus, 1 g of loaded with urea and dried LB60/PAAm40/FA0.062 hydrogel may release up to 2.7 g of urea on the first day and gradually up to 8.4 g of urea within 10 days. These amounts cover urea demand for agriculture fields[65] and can be easily controlled at the stage of hydrogel swelling in urea solution.

Furthermore, the presented data on cumulative urea release refer to the deionized water as a model medium. According to the comparative studies,[66] the urea release rate into the soil is significantly slower than in water, suggesting that obtained hydrogels will possess prolonged release in natural conditions.

Among other biopolymers such as cellulose, starch, alginate, pectin, etc., lignin is the most promising raw material for hydrogel production as it has the lowest rate of biodegradation in soil.[67] As reported previously, lignin degrades in nature mainly due to oxidative enzymes produced by white-rot fungi. This, in turn, leads to depolymerization and aromatic ring cleavage of lignins.[68] However, this process is slow and

depends greatly on the lignin origin and incubation medium.[69] Polyacrylamide also possesses significant resistance to microbial degradation but other degradation pathways, including mechanical, thermal, chemical, and photolytic (photocatalytic) may occur in soil and lead to the formation of hazardous compounds such as acrylamide or PAAm oligomers provoking serious environmental risks.[70] Therefore, the utilization of semisynthetic hydrogels with the lowest content of PAAm is considered to be an effective strategy for sustainable agriculture.

The weight loss of lignin-derived hydrogels LB60/PAAm40/FA0.042 and LB60/PAAm40/FA0.062 during incubation in soil for 40 days is presented in Figure 5d. After 40 days of incubation, there was a 9.5% weight loss for the LB60/PAAm40/FA0.062 hydrogels and a 14.4% weight loss for the LB60/PAAm40/FA0.042 hydrogels. As the biodegradation test was carried out within a short period, linear extrapolation given in Figure 5e gives a rough prediction of the weight loss of hydrogels over a longer period. Thus, after 6 months, an estimated mass of LB60/PAAm40/FA0.042 hydrogel will be 29% of the initial weight, and for LB60/PAAm40/FA0.062, it will be 53%.

The comparison of FTIR spectra of the hydrogel before and after incubation in soil (Figure S2) confirms the oxidative mechanism of lignin-derived hydrogel degradations. One can observe slightly increased intensity of peaks at 1268 cm^{-1} (C═O stretching in guaiacyl unit), 1218 cm^{-1} (C−C, C−O, and C═O stretching), 1140 cm^{-1} (C═O stretching), and 1030 cm^{-1} (C−O stretching), indicating the formation of carboxylic groups or other oxidized moieties.

The mechanical strength of lignin-derived hydrogels was assessed by employing storage modulus G'' and loss modulus G'' as a quantitative expression of the viscoelastic and rheological properties of the hydrogels. First, the stress sweep was performed at a fixed frequency of 1.0 Hz to determine the linear viscoelastic region of each hydrogel sample (Figure S3). Then, the dependence of dynamic moduli on the radial frequency was investigated, as shown in Figure 5f. It illustrates a typical picture of a well-developed elastic polymer network with storage modulus significantly exceeding loss modulus values. Thus, the storage modulus for LB60/PAAm40/FA0.042 makes 2500 Pa while sample LB60/PAAm40/FA0.062 with a higher cross-linking density showed a value of 3500 Pa.

In conclusion, chemically cross-linked hydrogels based on lignin and polyacrylamide were successfully prepared in this work. The proposed synthetic approach utilizes formaldehyde as a cross-linker and allows the adjustment of hydrogel performance characteristics in a wide range due to the change of hydrogel composition and cross-linking density. Hydrogel samples containing 60% lignin and 40% polyacrylamide showed an equilibrium swelling capacity of 235 g g^{-1} and 150 g g^{-1} depending on the cross-linking density. The results of the water retention test confirmed that 2.5% of the lignin-derived hydrogels ensures 10% to 19% higher moisture content in the soil after 8 days in conditions simulating drought stress compared to the substrate without hydrogel conditioner. Moreover, synthesized hydrogels are promising for fertilizer formulations with the ability to sustain the release of fertilizers. Thus, hydrogels (60% lignin and 40% polyacrylamide) previously loaded with urea release 81−89% of fertilizer within 7−8 days under laboratory conditions. Meanwhile, the cumulative release of unencapsulated urea reaches 97% within 1 h. Finally, the biodegradation rate in soil resulted in 10−15% weight loss after 40 days. Linear extrapolation of experimental data revealed that, after 200 days of incubation in soil, lignin-derived hydrogels would have from 45% to 70% weight loss depending on the cross-linking density.

Therefore, lignin-based hydrogels can potentially be used as soil conditioners and fertilizer formulations in agriculture, and the proposed synthetic approach can be utilized to effectively tailor the hydrogel properties.

■ ASSOCIATED CONTENT

Supporting Information

The Supporting Information is available free of charge at https://pubs.acs.org/doi/10.1021/acsagscitech.5c00084.

Swelling kinetic fitting curves in coordinates of the Fickian model, FTIR spectra of lignin-derived hydrogel before and after incubation in soil for 40 days, and amplitude sweep for hydrogel LB60/PAAm40/FA0.062 (PDF)

■ AUTHOR INFORMATION

Corresponding Author

Tetyana Budnyak − *Division of Nanotechnology and Functional Materials, Department of Materials Science and Engineering, The Ångström Laboratory, Uppsala University, Uppsala 751 03, Sweden; Department of Earth Sciences and Wallenberg Initiative Materials Science for Sustainability, Department of Earth Sciences, Uppsala University, Uppsala 752 36, Sweden;* orcid.org/0000-0003-2112-9308; Email: tetyana.budnyak@geo.uu.se

Author

Nataliia Fihurka − *Division of Nanotechnology and Functional Materials, Department of Materials Science and Engineering, The Ångström Laboratory, Uppsala University, Uppsala 751 03, Sweden*

Complete contact information is available at: https://pubs.acs.org/10.1021/acsagscitech.5c00084

Notes

The authors declare the following competing financial interest(s): The authors declare that they have filed a Swedish patent application for the hydrogel composition for soil improvement and have an interest in the exploitation of the results reported in this paper.

■ ACKNOWLEDGMENTS

This research was financed by the Swedish Foundation for Strategic Research (project no. UKR22-0062). This work was partially supported by the Wallenberg Initiative Materials Science for Sustainability (WISE), funded by the Knut and Alice Wallenberg Foundation.

■ REFERENCES

(1) Abobatta, W. Impact of Hydrogel Polymer in Agricultural Sector. *Advances in Agriculture and Environmental Science: Open Access (AAEOA)* **2018**, *1* (2), 59−64.

(2) Hussien, R. A.; Donia, A. M.; Atia, A. A.; El-Sedfy, O. F.; El-Hamid, A. R. A.; Rashad, R. T. Studying Some Hydro-Physical Properties of Two Soils Amended with Kaolinite-Modified Cross-Linked Poly-Acrylamides. *Catena (Amst)* **2012**, *92*, 172−178.

(3) Tariq, Z.; Iqbal, D. N.; Rizwan, M.; Ahmad, M.; Faheem, M.; Ahmed, M. Significance of Biopolymer-Based Hydrogels and Their

Applications in Agriculture: A Review in Perspective of Synthesis and Their Degree of Swelling for Water Holding. *RSC Adv.* **2023**, *13* (35), 24731−24754.
(4) Xiao, X.; Yu, L.; Xie, F.; Bao, X.; Liu, H.; Ji, Z.; Chen, L. One-Step Method to Prepare Starch-Based Superabsorbent Polymer for Slow Release of Fertilizer. *Chem. Eng. J.* **2017**, *309*, 607−616.
(5) Kareem, S. A.; Dere, I.; Gungula, D. T.; Andrew, F. P.; Saddiq, A. M.; Adebayo, E. F.; Tame, V. T.; Kefas, H. M.; Joseph, J.; Patrick, D. O. Synthesis and Characterization of Slow-Release Fertilizer Hydrogel Based on Hydroxy Propyl Methyl Cellulose, Polyvinyl Alcohol, Glycerol and Blended Paper. *Gels* **2021**, *7* (4), 262.
(6) Khushbu; Warkar, S. G.; Kumar, A. Synthesis and Assessment of Carboxymethyl Tamarind Kernel Gum Based Novel Superabsorbent Hydrogels for Agricultural Applications. *Polymer (Guildf)* **2019**, *182*, No. 121823.
(7) Jeong, D.; Kim, C.; Kim, Y.; Jung, S. Dual Crosslinked Carboxymethyl Cellulose/Polyacrylamide Interpenetrating Hydrogels with Highly Enhanced Mechanical Strength and Superabsorbent Properties. *Eur. Polym. J.* **2020**, *127*, No. 109586.
(8) Ribeiro, A. B.; Moreira, H.; Pereira, S. I. A.; Godinho, M.; Sousa, A. S. da S.; Castro, P.; Pereira, C. F.; Casanova, F.; Freixo, R.; Pintado, M. E.; Ramos, Ó. L. Bio-Based Superabsorbent Hydrogels for Nutrient Release. *J. Environ. Chem. Eng.* **2024**, *12* (2), No. 112031.
(9) Zainal, S. H.; Mohd, N. H.; Suhaili, N.; Anuar, F. H.; Lazim, A. M.; Othaman, R. Preparation of Cellulose-Based Hydrogel: A Review. *Journal of Materials Research and Technology* **2021**, *10*, 935−952.
(10) Xiao, X.; Yu, L.; Xie, F.; Bao, X.; Liu, H.; Ji, Z.; Chen, L. One-Step Method to Prepare Starch-Based Superabsorbent Polymer for Slow Release of Fertilizer. *Chem. Eng. J.* **2017**, *309*, 607−616.
(11) Youxin, Z.; Zhen, F.; Yurong, C.; Xianxing, H.; Sheng, Z.; Shuchen, S.; Xiaofei, T. A Bio-Based Hydrogel Derived from Moldy Steamed Bread as Urea-Formaldehyde Loading for Slow-Release and Water-Retention Fertilizers. *ACS Omega* **2021**, *6* (49), 33462−33469.
(12) Bai, C.; Zhang, S.; Huang, L.; Wang, H.; Wang, W.; Ye, Q. Starch-Based Hydrogel Loading with Carbendazim for Controlled-Release and Water Absorption. *Carbohydr. Polym.* **2015**, *125*, 376−383.
(13) Thakur, S.; Arotiba, O. A. Synthesis, Swelling and Adsorption Studies of a PH-Responsive Sodium Alginate−Poly(Acrylic Acid) Superabsorbent Hydrogel. *Polym. Bull.* **2018**, *75* (10), 4587−4606.
(14) Bukartyk, M.; Nosova, N.; Maikovych, O.; Bukartyk, N.; Stasiuk, A.; Dron, I.; Fihurka, N.; Khomyak, S.; Ostapiv, D.; Vlizlo, V.; Samaryk, V.; Varvarenko, S. Preparation and Research of Properties of Combined Alginate/Gelatin Hydrogels. *Journal of Chemistry and Technologies* **2022**, *30* (1), 11−20.
(15) Ghobashy, M. M.; El-Damhougy, B. Kh.; Nady, N.; El-Wahab, H. A.; Naser, A. M.; Abdelhai, F. Radiation Crosslinking of Modifying Super Absorbent (Polyacrylamide/Gelatin) Hydrogel as Fertilizers Carrier and Soil Conditioner. *J. Polym. Environ* **2018**, *26* (9), 3981−3994.
(16) Maikovych, O.; Nosova, N.; Bukartyk, N.; Fihurka, N.; Ostapiv, D.; Samaryk, V.; Pasetto, P.; Varvarenko, S. Gelatin-Based Hydrogel with Antiseptic Properties: Synthesis and Properties. *Appl. Nanosci* **2023**, *13* (12), 7611−7623.
(17) Dron, I.; Nosova, N.; Fihurka, N.; Bukartyk, N.; Nadashkevych, Z.; Varvarenko, S.; Samaryk, V. Investigation of Hydrogel Sheets Based on Highly Esterified Pectin. *Chemistry & Chemical Technology* **2022**, *16* (2), 220−226.
(18) Fang, S.; Wang, G.; Xing, R.; Chen, X.; Liu, S.; Qin, Y.; Li, K.; Wang, X.; Li, R.; Li, P. Synthesis of Superabsorbent Polymers Based on Chitosan Derivative Graft Acrylic Acid-Co-Acrylamide and Its Property Testing. *Int. J. Biol. Macromol.* **2019**, *132*, 575−584.
(19) Fang, S.; Wang, G.; Xing, R.; Chen, X.; Liu, S.; Qin, Y.; Li, K.; Wang, X.; Li, R.; Li, P. Synthesis of Superabsorbent Polymers Based on Chitosan Derivative Graft Acrylic Acid-Co-Acrylamide and Its Property Testing. *Int. J. Biol. Macromol.* **2019**, *132*, 575−584.
(20) Kaur, P.; Agrawal, R.; Pfeffer, F. M.; Williams, R.; Bohidar, H. B. Hydrogels in Agriculture: Prospects and Challenges. *J. Polym. Environ* **2023**, *31* (9), 3701−3718.
(21) José Borges Gomes, F.; de Souza, R. E.; Brito, E. O.; Costa Lelis, R. C. A Review on Lignin Sources and Uses. *Journal of Applied Biotechnology & Bioengineering* **2020**, 100−105.
(22) Yu, O.; Kim, K. H. Lignin to Materials: A Focused Review on Recent Novel Lignin Applications. *Applied Sciences* **2020**, *10* (13), 4626.
(23) Li, P.; Ren, J.; Jiang, Z.; Huang, L.; Wu, C.; Wu, W. Review on the Preparation of Fuels and Chemicals Based on Lignin. *RSC Adv.* **2022**, *12* (17), 10289−10305.
(24) Tkachenko, O.; Nikolaichuk, A.; Fihurka, N.; Backhaus, A.; Zimmerman, J. B.; Strømme, M.; Budnyak, T. M. Kraft Lignin-Derived Microporous Nitrogen-Doped Carbon Adsorbent for Air and Water Purification. *ACS Appl. Mater. Interfaces* **2024**, *16* (3), 3427−3441.
(25) Dudarko, O.; Budnyak, T.; Tkachenko, O.; Agback, T.; Agback, P.; Bonnet, B.; Ahrens, L.; Daniel, G.; Seisenbaeva, G. Removal of Poly- and Perfluoroalkyl Substances from Natural and Wastewater by Tailored Silica-Based Adsorbents. *ACS ES&T Water* **2024**, *4* (4), 1303−1314.
(26) Bajpai, P. *Biermann's Handbook of Pulp and Paper*; Elsevier, 2018; DOI: 10.1016/C2017-0-00513-X.
(27) Chen, H. Lignocellulose Biorefinery Feedstock Engineering. In *Lignocellulose Biorefinery Engineering*; Elsevier, 2015; pp 37−86; DOI: 10.1016/B978-0-08-100135-6.00003-X.
(28) Liu, J.; Li, X.; Li, M.; Zheng, Y. Lignin Biorefinery: Lignin Source, Isolation, Characterization, and Bioconversion. In *Advances in Bioenergy*; 2022; pp 211−270; DOI: 10.1016/bs.aibe.2022.05.004.
(29) Zerpa, A.; Pakzad, L.; Fatehi, P. Hardwood Kraft Lignin-Based Hydrogels: Production and Performance. *ACS Omega* **2018**, *3* (7), 8233−8242.
(30) El-Zawawy, W. K.; Ibrahim, M. M. Preparation and Characterization of Novel Polymer Hydrogel from Industrial Waste and Copolymerization of Poly(Vinyl Alcohol) and Polyacrylamide. *J. Appl. Polym. Sci.* **2012**, *124* (5), 4362−4370.
(31) El-Zawawy, W. K. Preparation of Hydrogel from Green Polymer. *Polym. Adv. Technol.* **2005**, *16* (1), 48−54.
(32) Farhat, W.; Venditti, R.; Mignard, N.; Taha, M.; Becquart, F.; Ayoub, A. Polysaccharides and Lignin Based Hydrogels with Potential Pharmaceutical Use as a Drug Delivery System Produced by a Reactive Extrusion Process. *Int. J. Biol. Macromol.* **2017**, *104*, 564−575.
(33) Poursorkhabi, V.; Misra, M.; Mohanty, A. K. Extraction of Lignin from a Coproduct of the Cellulosic Ethanol Industry and Its Thermal Characterization. *Bioresources* **2013**, *8* (4), 5083.
(34) Kong, F.; Wang, S.; Gao, W.; Fatehi, P. Novel Pathway to Produce High Molecular Weight Kraft Lignin−Acrylic Acid Polymers in Acidic Suspension Systems. *RSC Adv.* **2018**, *8* (22), 12322−12336.
(35) Argyropoulos, D. S.; Pajer, N.; Crestini, C. Quantitative 31P NMR Analysis of Lignins and Tannins. *J. Visualized Exp.* **2021**, No. 174, e62696.
(36) Song, B.; Liang, H.; Sun, R.; Peng, P.; Jiang, Y.; She, D. Hydrogel Synthesis Based on Lignin/Sodium Alginate and Application in Agriculture. *Int. J. Biol. Macromol.* **2020**, *144*, 219−230.
(37) Grytsenko, O.; Pukach, P.; Suberlyak, O.; Shakhovska, N.; Karovič, V., Jr. Usage of Mathematical Modeling and Optimization in Development of Hydrogel Medical Dressings Production. *Electronics (Basel)* **2021**, *10* (5), 620.
(38) Schott, H. Kinetics of Swelling of Polymers and Their Gels. *J. Pharm. Sci.* **1992**, *81* (5), 467−470.
(39) Tanan, W.; Panichpakdee, J.; Suwanakood, P.; Saengsuwan, S. Biodegradable Hydrogels of Cassava Starch-g-Polyacrylic Acid/Natural Rubber/Polyvinyl Alcohol as Environmentally Friendly and Highly Efficient Coating Material for Slow-Release Urea Fertilizers. *Journal of Industrial and Engineering Chemistry* **2021**, *101*, 237−252.
(40) Versino, F.; Urriza, M.; García, M. A. Eco-Compatible Cassava Starch Films for Fertilizer Controlled-Release. *Int. J. Biol. Macromol.* **2019**, *134*, 302−307.
(41) Suota, M. J.; da Silva, T. A.; Zawadzki, S. F.; Sassaki, G. L.; Hansel, F. A.; Paleologou, M.; Ramos, L. P. Chemical and Structural

Characterization of Hardwood and Softwood LignoForce™ Lignins. *Ind. Crops Prod* **2021**, *173*, No. 114138.
(42) Li, C.; Zhao, X.; Wang, A.; Huber, G. W.; Zhang, T. Catalytic Transformation of Lignin for the Production of Chemicals and Fuels. *Chem. Rev.* **2015**, *115* (21), 11559−11624.
(43) Samaryk, V.; Varvarenko, S.; Nosova, N.; Fihurka, N.; Musyanovych, A.; Landfester, K.; Popadyuk, N.; Voronov, S. Optical Properties of Hydrogels Filled with Dispersed Nanoparticles. *Chemistry & Chemical Technology* **2017**, *11* (4), 449−453.
(44) Nosova, N.; Samaryk, V.; Varvarenko, S.; Ferens, M.; Voronovska, A.; Nagornyak, M.; Khomyak, S.; Nadashkevych, Z.; Voronov, S. Porous Polyacrylamide Hydrogels: Preparation and Properties. *Voprosy Khimii i Khimicheskoi Tekhnologii* **2016**, No. 5−6, 78−86, DOI: 10.15421/jchemtech.v30i1.242230.
(45) Aufischer, G.; Kamm, B.; Paulik, C. Polycondensation of Kraft-Lignin toward Value-Added Biomaterials: Carbon Aerogels. *International Journal of Biobased Plastics* **2021**, *3* (1), 19−28.
(46) Huglin, M. B.; Radwan, M. A. Comparison of the Thermal Behaviour of Aqueous Solutions and Hydrogels of Poly(N-Methylol Acrylamide). *Polymer (Guildf)* **1991**, *32* (18), 3381−3386.
(47) Murugan, R.; Mohan, S.; Bigotto, A. FTIR and Polarized Raman Spectra of Acrylamide and Polyacrylamide. *Journal of the Korean Physical Society* **1988**, *32* (4), 505−512.
(48) Dumitrescu, A. M.; Lisa, G.; Iordan, A. R.; Tudorache, F.; Petrila, I.; Borhan, A. I.; Palamaru, M. N.; Mihailescu, C.; Leontie, L.; Munteanu, C. Ni Ferrite Highly Organized as Humidity Sensors. *Mater. Chem. Phys.* **2015**, *156*, 170−179.
(49) Meng, X.; Scheidemantle, B.; Li, M.; Wang, Y.; Zhao, X.; Toro-González, M.; Singh, P.; Pu, Y.; Wyman, C. E.; Ozcan, S.; Cai, C. M.; Ragauskas, A. J. Synthesis, Characterization, and Utilization of a Lignin-Based Adsorbent for Effective Removal of Azo Dye from Aqueous Solution. *ACS Omega* **2020**, *5* (6), 2865−2877.
(50) Herbert, H. L. *Lignins: Occurrence, Formation and Reactions*; Sarkanen, K. V., Ludwig, C. H., Eds.; John Wiley: New York, 1971.
(51) Magalhães, A. S. G.; Almeida Neto, M. P.; Bezerra, M. N.; Ricardo, N. M. P. S.; Feitosa, J. P. A. Application of Ftir in the Determination of Acrylate Content in Poly(Sodium Acrylate-Co-Acrylamide) Superabsorbent Hydrogels. *Quim. Nova* **2012**, *35* (7), 1464−1467.
(52) Murugan, R.; Mohan, S.; Bigotto, A. FTIR and Polarized Raman Spectra of Acrylamide and Polyacrylamide. *Journal of the Korean Physical Society* **1988**, *32* (4), 505−512.
(53) Zhang, X.; Han, M.; Fuseni, A.; Alsofi, A. M. An Approach to Evaluate Polyacrylamide-Type Polymers' Long-Term Stability under High Temperature and High Salinity Environment. *J. Pet Sci. Eng.* **2019**, *180*, 518−525.
(54) Zamani-Babgohari, F.; Irannejad, A.; Khayati, G. R.; Kalantari, M. Non-Isothermal Decomposition Kinetics of Commercial Polyacrylamide Hydrogel Using TGA and DSC Techniques. *Thermochim. Acta* **2023**, *725*, No. 179532.
(55) Salehi, M. B.; Moghadam, A. M.; Marandi, S. Z. Polyacrylamide Hydrogel Application in Sand Control with Compressive Strength Testing. *Pet Sci.* **2019**, *16* (1), 94−104.
(56) Amit, T. A.; Roy, R.; Raynie, D. E. Thermal and Structural Characterization of Two Commercially Available Technical Lignins for Potential Depolymerization via Hydrothermal Liquefaction. *Current Research in Green and Sustainable Chemistry* **2021**, *4*, No. 100106.
(57) Neamtu, I.; Chiriac, A. P.; Nita, L. E. Characterization of Poly(Acrylamide) as Temperature-Sensitive Hydrogel. *Journal of Optoelectronics and Advanced Materials* **2006**, *8* (5), 1.
(58) Khan, M. T. A.; Kwiczak-Yiğitbaşı, J.; Tootoonchian, P.; Morsali, M.; Lagzi, I.; Baytekin, B. Chemical Tracking of Temperature by Concurrent Periodic Precipitation Pattern Formation in Polyacrylamide Gels. *ACS Appl. Mater. Interfaces* **2022**, *14* (5), 7252−7260.
(59) Chen, Y.-C.; Chen, Y.-H. Thermo and PH-Responsive Methylcellulose and Hydroxypropyl Methylcellulose Hydrogels Containing K2SO4 for Water Retention and a Controlled-Release Water-Soluble Fertilizer. *Science of The Total Environment* **2019**, *655*, 958−967.
(60) Kareem, S. A.; Dere, I.; Gungula, D. T.; Andrew, F. P.; Saddiq, A. M.; Adebayo, E. F.; Tame, V. T.; Kefas, H. M.; Joseph, J.; Patrick, D. O. Synthesis and Characterization of Slow-Release Fertilizer Hydrogel Based on Hydroxy Propyl Methyl Cellulose, Polyvinyl Alcohol, Glycerol and Blended Paper. *Gels* **2021**, *7* (4), 262.
(61) Fernández-Pérez, M.; Garrido-Herrera, F. J.; González-Pradas, E.; Villafranca-Sánchez, M.; Flores-Céspedes, F. Lignin and Ethylcellulose as Polymers in Controlled Release Formulations of Urea. *J. Appl. Polym. Sci.* **2008**, *108* (6), 3796−3803.
(62) Maghsoodi, M. R.; Najafi, N.; Reyhanitabar, A.; Oustan, S. Hydroxyapatite Nanorods, Hydrochar, Biochar, and Zeolite for Controlled-Release Urea Fertilizers. *Geoderma* **2020**, *379*, No. 114644.
(63) Xiao, X.; Yu, L.; Xie, F.; Bao, X.; Liu, H.; Ji, Z.; Chen, L. One-Step Method to Prepare Starch-Based Superabsorbent Polymer for Slow Release of Fertilizer. *Chem. Eng. J.* **2017**, *309*, 607−616.
(64) Xiao, X.; Yu, L.; Xie, F.; Bao, X.; Liu, H.; Ji, Z.; Chen, L. One-Step Method to Prepare Starch-Based Superabsorbent Polymer for Slow Release of Fertilizer. *Chem. Eng. J.* **2017**, *309*, 607−616.
(65) Pinton, R.; Tomasi, N.; Zanin, L. Molecular and Physiological Interactions of Urea and Nitrate Uptake in Plants. *Plant Signal Behav* **2016**, *11* (1), No. e1076603.
(66) Kareem, S. A.; Dere, I.; Gungula, D. T.; Andrew, F. P.; Saddiq, A. M.; Adebayo, E. F.; Tame, V. T.; Kefas, H. M.; Joseph, J.; Patrick, D. O. Synthesis and Characterization of Slow-Release Fertilizer Hydrogel Based on Hydroxy Propyl Methyl Cellulose, Polyvinyl Alcohol, Glycerol and Blended Paper. *Gels* **2021**, *7* (4), 262.
(67) Adjuik, T. A.; Nokes, S. E.; Montross, M. D. Biodegradability of Bio-based and Synthetic Hydrogels as Sustainable Soil Amendments: A Review. *J. Appl. Polym. Sci.* **2023**, *140* (12), e53655.
(68) de Gonzalo, G.; Colpa, D. I.; Habib, M. H. M.; Fraaije, M. W. Bacterial Enzymes Involved in Lignin Degradation. *J. Biotechnol.* **2016**, *236*, 110−119.
(69) Tuomela, M. Biodegradation of Lignin in a Compost Environment: A Review. *Bioresour. Technol.* **2000**, *72* (2), 169−183.
(70) Xiong, B.; Loss, R. D.; Shields, D.; Pawlik, T.; Hochreiter, R.; Zydney, A. L.; Kumar, M. Polyacrylamide Degradation and Its Implications in Environmental Systems. *NPJ. Clean Water* **2018**, *1* (1), 17.